Geomechanics and Engineering, *Vol. 43, No. 5 (2025) 369-378*
https://doi.org/10.12989/gae.2025.43.5.369

Reliability-based optimization of MSE walls considering internal stability

Zafar Mahmood[1a], Mohsin Usman Qureshi[*2], Ali Murtaza Rasool[3b] and Syed Bilal Ahmed Zaidi[4c]

[1]*Department of Civil Engineering, Imam Mohammad Ibn Saud Islamic University, Riyadh, Saudi Arabia*
[2]*Faculty of Engineering, Sohar University, Sohar, Oman*
[3]*National Engineering Services Pakistan, Lahore, Pakistan*
[4]*University of Engineering and Technology Taxila, Taxila, Pakistan*

(*Received September 19, 2024, Revised November 11, 2025, Accepted November 12, 2025*)

Abstract. This study presents a reliability-based optimization (RBO) framework for the internal stability of mechanically stabilized earth walls, addressing reinforcement rupture and pullout limit states. The target reliability is set to β = 3.09 (P_f = 10^{-3}). The MSE wall, reinforced with steel strips, founded on cohesionless soil, with horizontal backfill and uniform live traffic surcharge is considered. Uncertain variables in rupture and pullout limit states are unit weight and friction angle of backfill soil; uniform live surcharge load; and yield strength of steel strips. The reliability index is calculated by the first-order reliability method (FORM). Constrained optimization with linear approximation (COBYLA) is used for determination of reliability index and optimization of reinforcement length. For rupture, optimizing horizontal spacing at fixed vertical spacing yields designs that satisfy $\beta \geq 3.09$ at every depth with minimum factor of safety $FS_{RP} \approx 1.7$ to 1.8 and a near height-independent β–FS relationship. For pullout, optimizing strip length shows the required length-to-height ratio decreases with wall height and tighter vertical spacing: representative maxima of L/H are 1.27, 0.83, 0.5 for H = 10 m at vertical spacing S_v = 1, 0.75, 0.5 m; 1.01, 0.7, 0.48 for H = 15 m; and 0.83, 0.6, 0.43 for H = 20 , respectively. Across cases, designs meeting β = 3.09 deliver factor of safety $FS_{PO} \approx 2.10$ at critical depth, but no unique β–FS mapping emerges for pullout. The framework converges to β-compliant, materially efficient layouts and clarifies how wall height and reinforcement spacing jointly control optimal L/H for pullout while leaving rupture behavior chiefly governed by spacing rather than wall height.

Keywords: constrained optimization; first-order reliability method; internal stability; MSE wall; reliability-based optimization

1. Introduction

Geotechnical engineering systems are associated with inherent risks and uncertainties. For an effective sustainable design methodology, it's crucial to measure these uncertainties to rationalize the practice (Christian 2004, Phoon and Ching 2015). The typical deterministic approaches in geotechnical engineering fall short, as they do not adequately account for the inherent uncertainties of geotechnical materials (Baecher and Christian 2003). Furthermore, the empirical safety factors employed in traditional deterministic models are incapable of including the influence of uncertainties in design variables on the system's overall efficacy.

The uncertainties in the design of geotechnical systems are due to inherent uncertainties of applied loading, soil properties, and the models used in calculations. The Reliability-based design (RBD) emerges as an alternative to the traditional allowable stress design (ASD) method. RBD considers the inherent uncertainties while meeting the design requirements, optimizing the design parameters, and ensuring economic efficiency. Reliability-based optimization (RBO) serves as an advanced method for optimizing geotechnical design problems. This approach incorporates unavoidable uncertainties while adhering to predefined design criteria, such as cost-effectiveness, thereby ensuring a design that is both economical and reliable. Recent studies have further refined these methodologies, offering more robust and feasible solutions in presence of uncertainty (Dutta and Putcha 2020, Low 2020, Mahmood 2020, Meng *et al*. 2022, Schweckendiek 2021, Tang and Phoon 2018, Wang and Owens 2022, Zhang *et al.* 2019). The stability and behavior of retaining walls under various conditions have been reported in recent studies. Ilbagitaher and Alielahi (2024) assess the seismic vulnerability of shored MSE walls. Zheng and Li (2024) investigate earth pressure in vertical backfills through both experimental and numerical methods. Lim *et al.* (2023) highlight how groundwater drawdown impacts wall stability. Najafizadeh and Zad (2022) experimentally evaluate back-to-back anchored walls using double-plate anchors, offering a new perspective on improving wall stability with anchored systems. Forghani *et al.* (2024) study the design of high MSE walls on weak foundations, emphasizing the challenges of ensuring stability in poor ground conditions. Tahamtan *et al*. (2024) utilize a coupled Lagrangian-Eulerian simulation to assess damage rates in

∗Corresponding author, Associate Professor
E-mail: Mqureshi@su.edu.om
[a]Assistant Professor
[b]Senior Engineer
[c]Associate Professor

ISSN: 2005-307X (Print), 2092-6219 (Online)

cantilever RC walls with backfill soil, demonstrating the complex interactions between structures and surrounding soils during damage events.

The use of reliability-based analysis and design of Mechanically Stabilized Earth (MSE) walls represents a transformative step in geotechnical engineering (Bathurst *et al*. 2019, Bozorgzadeh *et al*. 2020). This approach emphasized the necessity of considering uncertainties inherent in material properties, construction methodologies, and environmental influences (Kashani *et al*. 2022). Reliability-based design transcends traditional deterministic models by introducing probabilistic assessments of failure risks, thereby offering a more in-depth and comprehensive perspective on external and internal stability. This methodology quantifies failure probabilities using statistical models, and enhancing the safety margin evaluations (Park *et al*. 2021). This approach addresses the complexities of internal stability in MSE walls, such as the soil-structure interaction, reinforcement behavior, and external factors like seismic forces (Safaee *et al*. 2021). Yalcin *et al*. (2019) have demonstrated how reliability-based methods augment the predictive accuracy of internal stability models, particularly under diverse and unpredictable conditions. This progressive approach not only improves the design's predictive reliability but also optimizes design parameters, striking a balance between cost-effectiveness and risk mitigation. By adopting reliability-based analysis, engineers gain access to advanced tools for predicting and managing the internal stability of MSE walls, allowing them to navigate the complex and often challenging environments in which these structures operate.

The aim of the present study is to find an optimum design of the MSE wall using constrained optimization considering the internal stability for a target reliability (or target failure probability). The target reliability of 3.09 corresponding to failure probability of 0.001 (or probability of a failure of 1 in 1000) is used, which reflects a moderate-consequence safety level commonly adopted for geotechnical engineering structures (Baecher and Christian 2003). The limit states of reinforcement pullout failure and rupture failure are checked. The first-order reliability method (FORM) is used to determine reliability index. Constrained optimization with linear approximation (COBYLA) and reliability index calculation is implemented in Python language and Open TURNS (Baudin *et al*. 2016, Open TURNS 2021), open-source software for probabilistic modeling and uncertainty management.

2. Methodology

A formulation of reliability-based optimization is described in this section. Calculation of reliability index, constrained optimization algorithm, uncertainty variables, and limit state equations are described.

2.1 Reliability index

The reliability index can be used to express the stability of engineering systems in presence of inherent uncertainty of input variables related to material properties and loads. Hasofer and Lind (1974) defined the reliability index β as "the shortest distance from the mean value point of the random variables to the limit state surface, which can be expressed as follows

$$\beta = \min_{x \in F} \sqrt{(x-\mu)^T C^{-1} (x-\mu)} \tag{1}$$

where x is the vector of random variables μ is the vector of mean values, F is the failure domain, and C is the covariance matrix.

Random variables may not be normally distributed in many engineering problems. These non-normal random variables can be transformed from physical space to normal independent variables in the standard space (Hohenbichler and Rackwitz 1981, Liu and Der Kiureghian 1986, Low and Tang 2007, Lu *et al.* 2017, 2020).

The reliability index β in the standard space U can be calculated by finding the most probable point u^* by minimizing $u^T u = \sum_{i=1}^{n} u_i^2$ for the constraint $G(u) = 0$, where $G(u)$ is the limit state function in standard normal space. Therefore, β can be defined as the minimum distance from the origin of the standard normal space of random variable to the limit state surface at the failure point u^*, and can be expressed as follows

$$\beta = \min \sqrt{\mathrm{u}^{\mathrm{T}} u} = min \sqrt{\sum_{i=1}^{n} u_i^2} = min \sqrt{(u^*)^T u^*} \tag{2}$$

where u_i = transformed random variable in the standard normal space U. For normal and lognormal distributions respectively, relation between random variable x_i and its transformed version can be expressed by Eqs. (3) and (4) (Low and Tang 2007).

$$x_i = \mu_i + u_i \sigma_i \tag{3}$$

$$x_i = \exp[\lambda + \zeta u_i], \quad \zeta = \sqrt{\ln[1 + (\sigma_i/\mu_i)^2]}, \ \& \ \lambda = \ln \mu_i - 0.5\zeta^2 \tag{4}$$

where μ_i and σ_i are the mean and standard deviation of random variable x_i respectively.

2.2 Constrained optimization

Constrained optimization with linear approximation (COBYLA) is a gradient-free capable of handling equality and inequality constraints, and well-suited to nonlinear, nonsmooth, or implicitly defined constrains (Powell 1994, 1998). It is a technique of finding a vector x that is local minimum to a scalar function $f(x)$ subject to constraints on the allowable x

$$\min_x f(x) \text{ such that } \begin{cases} g(x) = 0 \\ h(x) \geq 0 \\ lb \leq x \leq ub \end{cases} \tag{5}$$

where $g(x)$, $h(x)$ are equality and inequality constraints; lb, ub are upper and lower bounds; and $f(x)$ is the objective function that returns a scalar. Open TURNS (Baudin *et al.* 2016, Open TURNS 2021) which is an open-source software for probabilistic modeling and uncertainty management, is used to implement COBYLA algorithm.

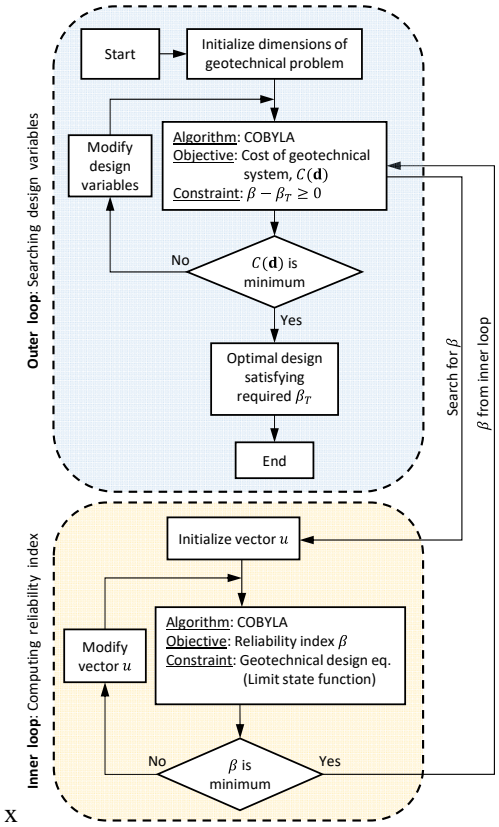

Fig. 1 Flow chart for reliability-based optimization

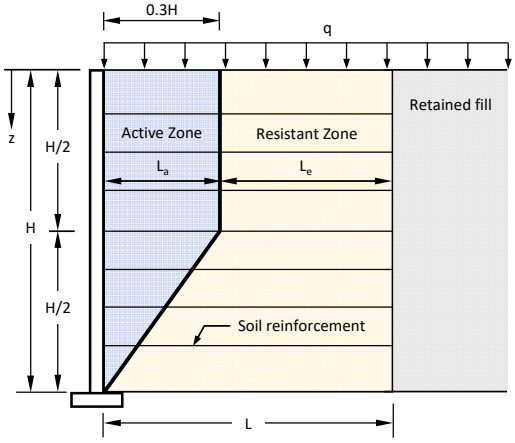

Fig. 2 Failure wedge for the internal stability of MSE wall

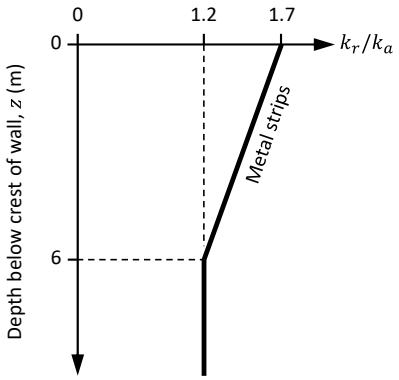

Fig. 3 Variation of the coefficient of lateral stress ratio k_r/k_a with depth

2.3 Process of optimization

Optimizing the cost of a geotechnical system, while satisfying the design requirements and target reliability β_{Target} is a constrained optimization problem (e.g, see (Eq. (16)) as objective for pullout limit sate). RBO can be considered as a multi-objective optimization problem since the determination of reliability index is itself an optimization problem (Mahmood 2020). Fig. 1 shows the process of optimization. In the outer loop, the design variables are explored to minimize the cost of geotechnical system considering target reliability as constraint. Design variables are updated to minimize cost, and iterations continue until the objective change and the active-constraint violation (i.e., $\beta_{target} - \beta$, if any) are each below 1×10^{-6}. In the inner loop, reliability index is minimized considering design requirements as the constraint. For each candidate design, the FORM procedure iterates until both the change in β and the limit-state residual $G(u)$ fall below 1×10^{-6}. This typically requires a few tens of function evaluations, ensuring accurate β values are supplied to the outer loop.

The constrained optimization uses COBYLA with a constraint tolerance of 1×10^{-6} and a maximum of 20,000 iterations. The trust-region step size is adapted automatically by the algorithm; thus, step lengths are not fixed but adjusted based on progress.

2.4 RBO of MSE wall considering internal stability

A schematic diagram and failure wedge for the internal stability of the MSE wall is shown in Fig. 2. The MSE Wall with horizontal backslope and uniform live traffic surcharge is considered.

The maximum tensile driving force acting on a steel strip is given by

$$T_{max} = (\gamma_R z + q) K_r S_v S_h \tag{6}$$

where γ_R is the unit weight of reinforced fill, z is the depth of steel strip below crest of MSE wall of height H, q is the continuous traffic surcharge load, S_v is vertical spacing of steel strips, S_h is the horizontal spacing of steel strips, K_r is the horizontal component of active lateral earth pressure coefficient which varies from $1.7K_a$ at the top of the wall to $1.2K_a$ at a depth of 6 m and remains constant thereafter (Fig. 3) and can be expressed as

$$\begin{aligned} K_r &= (1.7 - z/12)K_a \quad \text{for} \quad z \leq 6 \text{ m} \\ K_r &= 1.2K_a \quad \text{for} \quad z > 6 \text{ m} \end{aligned} \tag{7}$$

where $K_a$is coefficient of active earth pressure, calculated using the Rankine equation and peak friction angle of reinforced soil ϕ_R, expressed as $K_a = (1 - \sin\phi_R)/(1 + \sin\phi_R)$.

2.4.1 Limit state equation for pullout failure

The pullout driving force acting on a steel strip is given

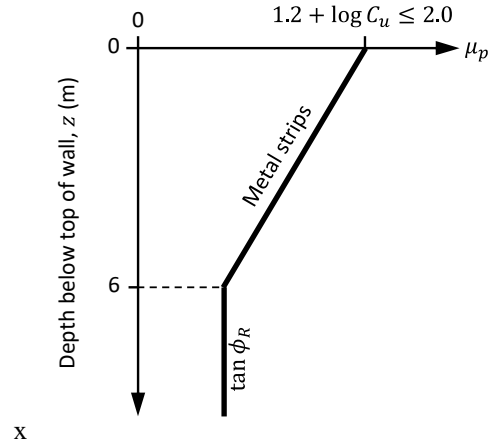

Fig. 4 Default values for pullout friction factor μ_p

by T_{max} in Eq (6). The pullout resisting force on a steel strip is given by

$$R_{PO} = 2.0 L_e b(\gamma_R z + q)\mu_p \tag{8}$$

where L_e is embedment length of steel strip in resistant zone, b is the width of steel strip, μ_p is empirical friction factor that varies from $1.2 + \log C_u \leq 2$ to $\tan \phi_R$ at a depth of 6 m and remains constant thereafter (Fig. 4) and can be expressed as

$$\begin{gathered} \mu_p = \mu_{p6} + (\mu_{p0} - \mu_{p6})(6 - z)/6 \quad \text{for } z \leq 6 \text{ m} \\ \mu_p = \mu_{p6} \quad \text{for } z > 6 \text{ m} \end{gathered} \tag{9}$$

where $\mu_{p0} = 1.2 + \log C_u \leq 2$ and $\mu_{p6} = \tan \phi_R$. The parameter C_u is the coefficient of uniformity of the reinforced soil.

The factor of safety against pullout failure at a depth z from crest of the wall is given as

$$FS_{PO} = \frac{R_{PO}}{T_{max}} = \frac{2.0 L_e b(\gamma_R z + q)\mu_p}{(\gamma_R z + q) K_r S_v S_h} \tag{10}$$

The limit state function for pullout failure at a depth z from crest of the wall is given as

$$\begin{aligned} G_1(\boldsymbol{x}) &= R_{PO} - T_{max} \\ &= 2.0 L_e b(\gamma_R z + q)\mu_p - (\gamma_R z + q) K_r S_v S_h \end{aligned} \tag{11}$$

2.4.2 Limit state equation for rupture failure

The long-term tensile resistance or rupture resistance of the steel strip is given as follows

$$T_{al} = f_y b(E_n - E_{dep}) \tag{12}$$

where f_y is the yield strength of steel, b is the width of steel strip, and E_n is the initial non-corroded nominal thickness of steel strip, and E_{dep} is depleted thickness during the design lifetime. Considering a zinc coating of 86 μm and the rate of loss of zinc coating as 15 μm per side per year for the first two years of service life and 4 μm per side for the rest of life (AASTHO 2014), the life of zinc coating is determined as 16 years. The rate of loss of carbon steel is 12 μm per side per year. The depleted thickness E_{dep} is calculated as

$$E_{dep} = 2V(t_{des} - t_{zinc}) \tag{13}$$

where V is the rate of loss of carbon steel (i.e., 12 μ_m per year per side), t_{des} is the design life, and t_{zinc} is the life of zinc coating (i.e., 16 years).

The factor of safety against rupture failure at a depth z from crest of the wall is given as

$$FS_{RP} = \frac{T_{al}}{T_{max}} = \frac{f_y b(E_n - E_{dep})}{(\gamma_R z + q) K_r S_v S_h} \tag{14}$$

The limit state function for pullout failure at a depth z from crest of the wall is given as

$$\begin{aligned} G_2(\boldsymbol{x}) &= T_{al} - T_{max} \\ &= f_y b(E_n - E_{dep}) - (\gamma_R z + q) K_r S_v S_h \end{aligned} \tag{15}$$

2.4.3 Assessment of uncertainties

Uncertain variables in rupture and pullout limit states are unit weight, friction angle, uniform live surcharge load and yield strength of steel strips, which are modeled as statistically independent (uncorrelated).

Uncertainty of unit weight: The coefficient of variation (COV) of the soil's unit weight, γ, reported in the literature ranges from 0.03 to 0.2 (Foye *et al*. 2006, Hummit 1966, Lacroix and Horn 1973, Basha and Babu 2010, Phoon and Kulhawy 1999, Wolff 1994). In this study, the unit weight is assumed to follow a normal distribution with a COV of 0.1 for reinforced soil.

Uncertainty of friction angle: The peak friction angle, ϕ, is used to estimate the active earth pressure coefficient and bearing capacity factors. The COV of ϕ reported in the literature ranges from 0.008 to 0.1 (Low 2005, Negussey *et al.* 1988, Verdugo and Ishihara 1996). In this study, friction angle is assumed to follow a lognormal distribution with a COV of 0.1.

Uncertainty of uniform live surcharge load: Since live loads have high uncertainty, therefore, surcharge load is assumed to follow lognormal distribution with a COV of 0.2.

Uncertainty of steel yield strength: Hess et al. (2002) reported the COV of different grades of steel from 0.026 to 0.11 with COV of high-strength steel as 0.091. In this study, steel yield strength is assumed to follow lognormal distribution with a COV of 0.09. Table 1 summarizes the distribution and statistics of these variables.

3. Illustrated example

Reliability-based optimization of a 20-m high MSE wall considering internal stability is investigated. MSE wall with horizontal backslope and live traffic surcharge is considered. Steel strips have initial (non-corroded) thickness 5 mm and 50 mm; a design life of 75 years is adopted. The thickness depletion over the design life is applied as described in Section 2.3.2; and all calculations in this section use the depleted thickness for resistance calculations.

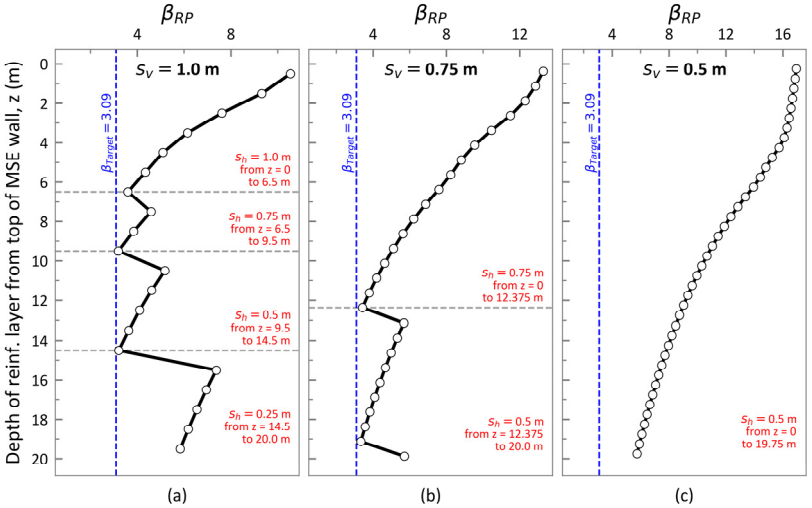

Fig. 5 Optimization results of 20-m high MSE wall for limit state of rupture. Variation of β with depth for different values of steel strip vertical spacing ranging from (a) S_v = 1 m, (b) S_v = 0.75 m, and (c) S_v = 0.5 m, respectively

Table 1 Distribution and statistics of uncertain variables

variable	Distribution	Mean	COV	Std. dev.
ϕ_R (°)	Lognormal	34	0.1	3.4
γ_R (kN/m^3)	Normal	18	0.1	1.8
f_y (MPa)	Lognormal	460	0.09	41.4
q (kPa)	Lognormal	12	0.2	2.4

Table 2 Optimization results for rupture failure

z (m)	S_h (m)
S_v = 1 m	
0 – 6.5	1
6.5 – 9.5	0.75
9.5 – 14.5	0.5
14.5 – 20	0.25
S_v = 0.75 m	
0 – 12.375	0.75
12.375 – 20	0.5
S_v = 0.5 m	
0 – 20	0.5

3.1 Optimization of steel strip spacing for rupture failure

From (Eqs. (14) and (15)) it is evident that limit state of rupture failure depends on steel strip location, steel strip cross section (i.e., thickness and width), steel strip inter-spacing (both horizontal and vertical), surcharge load, unit weight of reinforced fill, and friction angle of reinforced fill. Rupture failure does not depend on the steel strip length. Since strip cross section is constant, interspacing of reinforcement can be adjusted to obtain the required reliability index.

In the analysis, vertical spacing of steel strips is kept constant whereas the horizontal spacing is adjusted to obtain the desired reliability index for limit state of rupture. Analysis is done with three different values of vertical spacing i.e., 0.5, 0.75 and 1.0 m. The horizontal spacing is started with the value of constant vertical spacing from the crest of MSE wall. When the reliability index at a depth decreases below the target value, the horizontal spacing is reduced to meet the requirement of reliability.

The reliability index for rupture failure, β_{RP}, at every strip location is computed using Python 3.8 and open TURNS 1.16 (Baudin *et al*. 2016, Open TURNS 2021). Fig. 5 shows the optimization results of strip spacing considering rupture failure. Reliability index for rupture failure, β_{RP}, at every strip location is computed and plotted as shown in Fig. 5. Fig. 5(a) shows reliability index β_{RP} for constant vertical spacing S_v = 1 m. As the value of β_{RP} decreases below β_{Target} = 3.09, the horizontal spacing is decreased. If the horizontal spacing is kept as mentioned in the Fig. 5(a), and summarized in the Table 2, the calculated value of β_{RP} is always greater than β_{Target} at every steel strip location. Optimization results for vertical spacing of S_v = 0.75 m and S_v = 0. 5 m are shown in Figs. 5(b) and 5(c) respectively.

Fig. 6 shows the factor of safety against rupture at each strip location for the optimized spacing. The factor of safety is calculated from the average values of uncertain variables (Table 1). The minimum factor of safety against rupture failure, $(FS_{RP})_{Min.} > 1.7$, which corresponds to reliability index of β_{Target} = 3.09.

3.2 Optimization of steel strip length for pullout failure

From (Eqs. (10) and (11)) it is evident that limit state of pullout failure depends on steel strip location, steel strip width, steel strip length, steel strip inter-spacing (both horizontal and vertical), surcharge load, unit weight of reinforced fill, and friction angle of reinforced fill. Pullout failure does not depend on steel strip thickness. Steel strip length can be adjusted to obtain the required reliability index.

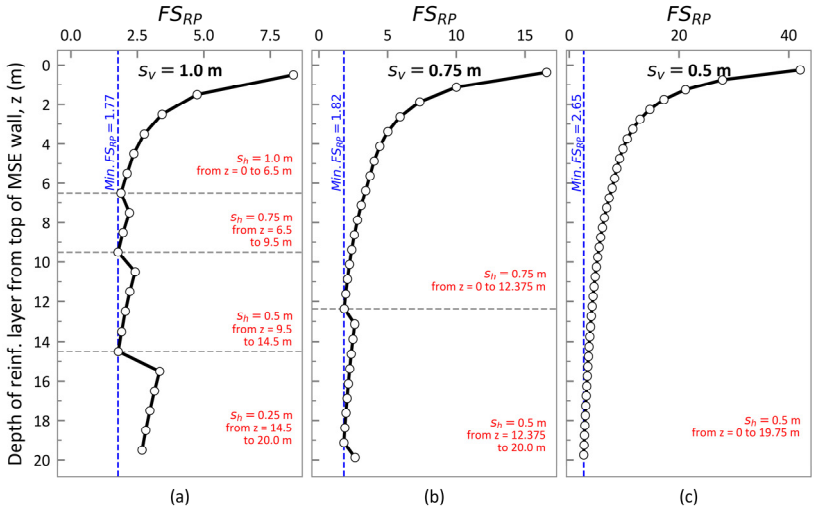

Fig. 6 Factor of safety against rupture for 20-m high MSE wall. Variation of FS with depth for different values of steel strip vertical spacing ranging from (a) S_v = 1 m, (b) S_v = 0.75 m, and (c) S_v = 0.5 m, respectively

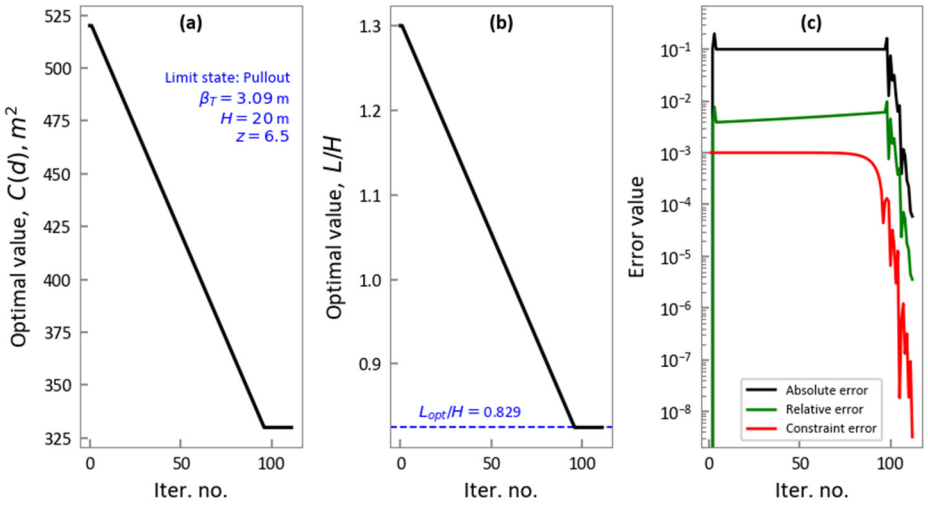

Fig. 7 Optimization results of 20-m high MSE wall, for steel strip located at z = 6.5 m, for limit state of pullout, for β_{Target} = 3.09. (a) Convergence of objective, (b) Convergence of L_{opt}/H, and (c) Evolution of absolute, relative error of objective and constraint error

Let the objective is to minimize the MSE wall area by changing the design variables $\boldsymbol{d} = \{L\}$. The design space is considered as $0.4H < L < 1.5H$. The optimization problem can be expressed as

$$\begin{aligned} &\min C(\boldsymbol{d}) = LH \\ &\text{Subject to } \beta_{PO} > \beta_{Target} \end{aligned} \tag{16}$$

where $C(\boldsymbol{d})$ is the area of MSE wall and β_{PO} is the reliability index for pullout failure. The constrained optimization function COBYLA is used for the double loop multi-objective constrained optimization problem. In the outer loop, the area of the MSE wall is optimized while the constraint is $\beta_{PO} - \beta_{Target} \geq 0$. In the inner loop, β_{PO} is minimized (Eq. (2)) while the limit state of pullout failure is the constraint.

The optimization of strip length is implemented in Python 3.8 and open TURNS 1.16 (Baudin *et al.* 2016, Open TURNS 2021). Fig. 7 shows the optimization results of strip length located at z = 6.5 m considering pullout failure. The horizontal and vertical spacing determined for rupture failure are used. Figs. 7(a) and 7(b) show the convergence of objective and L_{opt}/H respectively considering the reliability constraint $\beta_{PO} \geq \beta_{Target}$. Fig. 7(c) shows the evolution of absolute and relative error during the convergence of objective as well as constraint error ($\beta_{PO} - \beta_T$). The absolute error can be described as $|\xi_{n+1} - \xi_n|$, and the relative error can be described as $|\xi_{n+1} - \xi_n| / |\xi_{n+1}|$ where ξ_{n+1} and ξ_n are two consecutive approximations of the optimum. The algorithm continues until these errors are below 1×10^{-6}. (Note: β at each iterate is computed by the inner FORM procedure, which is converged per the criteria in Section 2.2). The process of strip length optimization is performed at each strip location.

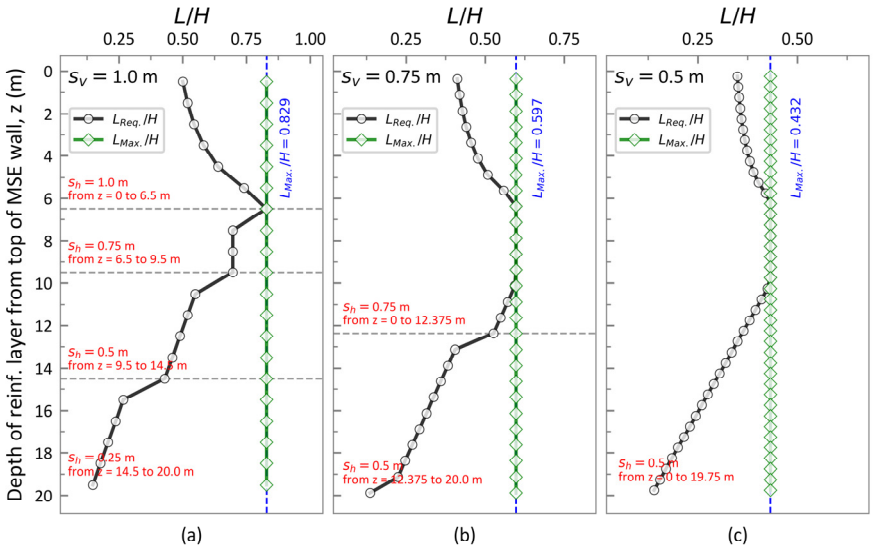

Fig. 8 Optimization results of 20-m high MSE wall for limit state of pullout for target reliability index of β_{Target} = 3.09. Variation of L/H ratio with depth for different values of steel strip vertical spacing ranging from (a) S_v = 1 m, (b) S_v = 0.75 m, and (c) S_v = 0.5 m, respectively

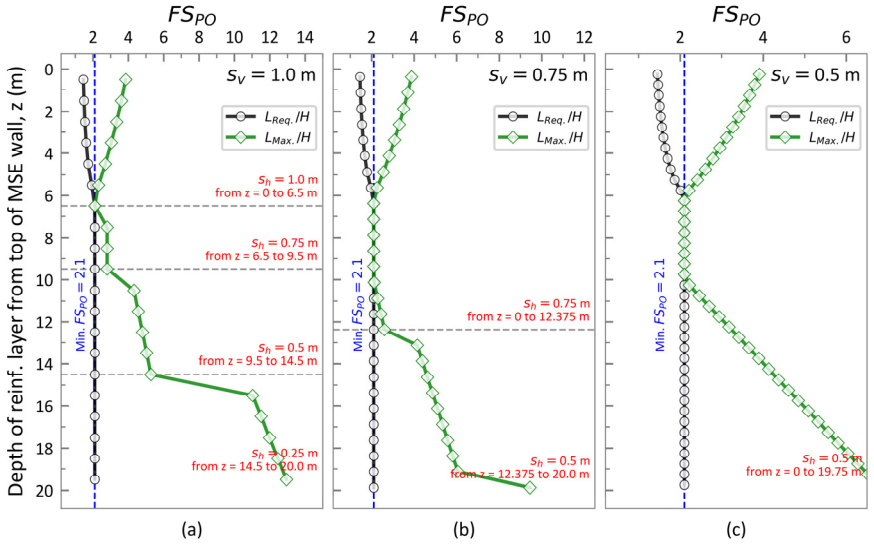

Fig. 9 Factor of safety against pullout for 20-m high MSE wall. Variation of factor of safety with depth for different values of steel strip vertical spacing ranging from (a) S_v = 1 m, (b) S_v = 0.75 m, and (c) S_v = 0.5 m, respectively

Fig. 8. Show the optimization results of strip length considering pullout failure. As seen in the Fig. 8, $L_{Req.}/H$, or ratio of required strip length to the MSE wall height, is determined at each strip location. The vertical spacing are kept as S_v= 1.0, 0.75, and 0.5 m respectively (Figs. 8(a)-8(c)). The horizontal spacing determined for the rupture failure are used. The detailed discussion is as follows.

- For S_v = 1.0 m, the ratio of maximum strip length to MSE wall height, $L_{Max.}/H$ = 0.829 at the depth z = 6.5 m for β_{Target} = 3.09. At other locations, the $L_{Req.}/H$ is less than 0.829.
- For S_v = 0.75 m, the ratio of maximum strip length to MSE wall height, $L_{Max.}/H$ = 0.598 at the depth z = 6.375 m to 9.375 m. At other locations, the $L_{Req.}/H$ is less than 0.598.
- For S_v = 0.5 m, the ratio of maximum strip length to MSE wall height, $L_{Max.}/H$ = 0.432 at the depth z = 6.25 m to 9.75 m. At other locations, the $L_{Req.}/H$ is less than 0.432.

Fig. 9 shows the factor of safety against pullout at each strip location for the optimized spacing for required strip length as well as maximum strip length. The factor of safety is calculated from the average values of uncertain variables (Table 1). The minimum factor of safety is same for all cases which corresponds to reliability index of β_{Target} = 3.09.

Table 3 Summary of optimization results for target reliability index of β_{Target} = 3.09 for MSE walls of different heights

S_v (m)	z (m)	S_h (m)	FS_{RP}	$L_{Max.}/H$	$L_{Max.}$ (m)	FS_{PO}
			H = 10 m			
1.0	0 – 6.5	1.0	1.77	1.267	12.7	2.10
	6.5 – 10	0.75				
0.75	0 – 10	0.75	1.79	0.830	8.3	2.10
0.5	0 – 10	0.5	5.18	0.495	4.95	1.92
			H = 15 m			
1.0	0 – 6.5	1.0	1.77	1.005	15.1	2.10
	6.5 – 9.5	0.75				
	9.5 – 15	0.5				
0.75	0 – 12.375	0.75	1.84	0.696	10.4	2.10
	12.375 – 15	0.5				
0.5	0 – 15	0.5	3.50	0.476	7.1	2.10
			H = 20 m			
1.0	0 – 6.5	1.0	1.77	0.829	16.6	2.10
	6.5 – 9.5	0.75				
	9.5 – 14.5	0.5				
	14.5 – 20	0.25				
0.75	0 – 12.375	0.75	1.82	0.597	12	2.10
	12.375 – 20	0.5				
0.5	0 – 20	0.5	2.65	0.432	8.6	2.10

3.3 Parametric study for different wall heights

Table 3 summarizes the optimization results for target reliability index of $\beta_{Targtet}$ = 3.09 for MSE wall heights ranging from 10 to 20 m. Inter-strip spacing and trip lengths are optimized for limiting states of rupture and pullout failures. The factor of safety against rupture failure (FS_{RP}) and pullout failure (FS_{PO}) are calculated from the mean values of uncertain variables. The insights can be summarized as follows:

- *Rupture*: At the β-optimal designs, the factor of safety FS_{RP} clusters around 1.7-1.8 when $S_v \geq 0.75$ m and increases with tighter S_v; the β-FS relation is effectively height-insensitive over H = 10-20 m.
- *Pullout*: β-optimal factor of safety FS_{PO} is ~2.1 in most cases, while L/H is jointly controlled by H and S_v, decreasing monotonically with taller H and tighter S_v.
- *Spacing architecture*: Enforcing $\beta \geq$3.09 pointwise with depth yields piecewise S_h. The optimizer tightens spacing locally where β dips, raising local reliability while avoiding over-conservatism where β already exceeds the target.

3.4 Limitations relative to prior works

Our findings are conditioned by the selected limit-state formulations, lateral stress representation, and statistical inputs (distribution types, and coefficients of variation) for a steel-strip MSE wall. The main limitations are: (i) *System specificity*: quantitative comparisons with geosynthetic (Bathurst *et al.* 2019) or steel-grid systems (Bathurst *et al.* 2021) are limited because pullout/rupture resistances and interface parameters differ by reinforcement type; (ii) *Model-form dependence*: the observed β –FS mapping; robust for rupture, non-unique for pullout; reflects the specific resistance/load models adopted here and is not universal; (iii) *Uncertainty characterization*: inputs reflect generic values and do not include project-specific calibration (construction variability, backfill scatter, facing stiffness), which could shift β and the optimized layouts; (iv) *Methodological scope*: reliability indices were computed using FORM and optimization targeted a single objective; alternative reliability methods (e.g., simulation-based) or multi-objective design (cost–serviceability–robustness) may yield different optima; (v) *Load cases*: seismic, time-dependent, and environmental effects were not treated and could alter reliability for certain systems.

4. Conclusions

We carried out reliability-based optimization (RBO) of the MSE wall considering internal stability by using constrained optimization with linear approximation (COBYLA). The limit states of rupture and pullout, corresponding to internal stability, are used. The MSE wall of Height H = 20 m founded on cohesionless soil with horizontal backfill and live traffic surcharge is studied. Mean and standard deviation values of uncertain values, used in the study, are those reported in the literature (Foye *et al.* 2006, Hess *et al*. 2002, Hummit 1966, Lacroix and Horn 1973, Low 2005, Basha and Babu 2010, Negussey *et*

al. 1988, Phoon and Kulhawy 1999, Verdugo and Ishihara 1996, Wolff 1994). The study findings are as follows.

i. Limit state of rupture failure depends on steel strip location, steel strip cross section, steel strip inter-spacing, surcharge load, unit weight of reinforced fill and friction angle of reinforced fill. Rupture failure does not depend on streel strip length.
ii. Limit state of pullout failure depends on steel strip location, steel strip width, steel strip length, steel strip inter-spacing, surcharge load, unit weight of reinforced fill, unit weight of reinforced fill, and friction angle of reinforced fill. Pullout failure does not depend on steel strip thickness.
iii. Keeping constant vertical spacing of steel strips, horizontal spacing can be adjusted for limit state of rupture failure, while the length of steel strip can be determined for limit state of pullout failure for a given value of target reliability.
iv. Required length-to-height ratios decrease with increasing H and with tighter vertical spacing S_v. Representative maxima of L/H at critical depth are 1.27, 0.83, 0.5 for H = 10 m at vertical spacing S_v = 1, 0.75, 0.5 m; 1.01, 0.7, 0.48 for H = 15 m; and 0.83, 0.6, 0.43 for H = 20 , respectively.

Overall, the RBO framework converged to β-compliant, materially efficient layouts, quantified how H and Sv jointly control optimal L/H for pullout, and clarified that rupture reliability is governed chiefly by reinforcement spacing with a stable, near height-invariant β-FS behavior under the adopted uncertainty models.

Acknowledgements

The authors would like to acknowledge Imam Mohammad Ibn Saud Islamic University, Riyadh, Saudi Arabia and Sohar University, Sohar, Oman for supporting this research.

Funding statement

The work is supported and funded by the Deanship of Scientific Research at Imam Mohammad Ibn Saud Islamic University (IMSIU) (grant number IMSIU-DDRSP2502).

References

AASTHO. (2014), LRFD Bridge Design Spesifications. In *American Association of State Highway and Transportation Officials, WA, D.C.*

Baecher, G.B. and Christian, J.T. (2003), *Reliability and statistics in geotechnical engineering*. John Wiley and Sons.

Basha, B.M. and Babu, G.L.S. (2010), "Reliability assessment of internal stability of reinforced soil structures: A pseudo-dynamic approach", *Soil Dyn. Earthq. Eng.*, **30**(5), 336-353. https://doi.org/10.1016/j.soildyn.2009.12.007.

Bathurst, R.J., Allen, T.M., Miyata, Y., Javankhoshdel, S. and Bozorgzadeh, N. (2019), "Performance-based analysis and design for internal stability of MSE walls", *Georisk*, **13**(3), 214-225. https://doi.org/10.1080/17499518.2019.1602879.

Bathurst, R.J., Bozorgzadeh, N., Miyata, Y. and Allen, T.M. (2021), "Reliability-based design and analysis for internal limit states of steel grid–reinforced mechanically stabilized earth walls", *Can. Geotech. J.*, **58**(5), 695-710. https://doi.org/10.1139/cgj-2019-0820.

Bathurst, R. J., Lin, P. and Allen, T. (2019), "Reliability-based design of internal limit states for mechanically stabilized earth walls using geosynthetic reinforcement", *Can. Geotech. J.*, **56**(6), 774-788. https://doi.org/10.1139/cgj-2018-0074.

Baudin, M., Dutfoy, A., Iooss, B. and Popelin, A.L. (2016), OpenTURNS: An Industrial Software for Uncertainty Quantification in Simulation, (Eds., R. Ghanem, D. Higdon and H. Owhadi), *Handbook of Uncertainty Quantification*, 1-38. Springer International Publishing. https://doi.org/10.1007/978-3-319-11259-6_64-1.

Bozorgzadeh, N., Bathurst, R.J. and Allen, T.M. (2020), "Influence of corrosion on reliability-based design of steel grid MSE walls", *Struct. Saf.*, **84**, 101914. https://doi.org/10.1016/j.strusafe.2019.101914.

Christian, J.T. (2004). "Geotechnical engineering reliability: How well do we know what we are doing?", *J. Geotech. Geoenviron. Eng.*, **130**(10), 985-1003. https://doi.org/10.1061/(ASCE)1090-0241(2004)130:10(985).

Dutta, S. and Putcha, C. (2020), "Reliability-based design optimization of a large-scale truss structure using polynomial chaos expansion metamodel", *Lecture Notes in Mechanical Engineering*, 481-488. https://doi.org/10.1007/978-981-13-9008-1_39.

Forghani, M., Panah, A.K. and Hamidi, S. (2024). "High MSE wall design on weak foundations", *Geomech. Eng.*, **36**(4), 329–341. https://doi.org/https://doi.org/10.12989/gae.2024.36.4.329

Foye, K.C., Salgado, R. and Scott, B. (2006), "Assessment of variable uncertainties for reliability-based design of foundations", *J. Geotech. Geoenviron. Eng.*, **132**(9), 1197-1207. https://doi.org/10.1061/(asce)1090-0241(2006)132:9(1197).

Hasofer, A.M. and Lind, N.C. (1974), An exact and invariant second-moment code format", *J. Eng. Mech. Div.*, **100**, 111-121.

Hess, P.E., Bruchman, D., Assakkaf, I.A. and Ayyub, B.M. (2002). "Uncertainties in material and geometric strength and load variables", *Naval Engineers J.*, **114**(2), 139-166. https://doi.org/10.1111/j.1559-3584.2002.tb00128.x.

Hohenbichler, M. and Rackwitz, R. (1981), "Non-normal dependent vectors in structural safety", *ASCE J Eng Mech Div*, **107**(6), 1227-1238. https://doi.org/10.1061/jmcea3.0002777.

Hummit, G.M. (1966), "Statistical analysis of data from a comparative laboratory test program sponsored by ACIL. No. AEWES-Misc Paper-4-785, Army Engineer Waterways Experiment Station VicksburgMs Geotechnical Lab, Vicksburg, MS, USA. In *U.S. Army Engineer Waterways Experiment Station.* (Issue 4). U.S. Army Engineer Waterways Experiment Station. https://hdl.handle.net/11681/35595.

Ilbagitaher, S. and Alielahi, H. (2024), "Seismic fragility assessment of shored mechanically stabilized earth walls", *Geomech. Eng.*, **36**(3), 277-293. https://doi.org/10.12989/gae.2024.36.3.277.

Kashani, A.R., Camp, C.V., Azizi, K. and Rostamian, M. (2022), "Multi-objective optimization of mechanically stabilized earth retaining wall using evolutionary algorithms", *Int. J. Numer. Anal. Method. Geomech.*, **46**(8), 1433-1465. https://doi.org/10.1002/nag.3352.

Lacroix, Y. and Horn, H.M. (1973), "Direct determination and indirect evaluation of relative density and its use on earthwork construction projects", (Eds., E.T. Selig and R.S. Ladd), *Evaluation of Relative Density and its Role in Geotechnical Projects Involving Cohesionless Soils*, 251-280. ASTM International. https://doi.org/10.1520/STP37877S.

Lim, H., Park, J., Kim, J. and Ko, J. (2023), "Numerical study on

stability and deformation of retaining wall according to groundwater drawdown", *Geomech. Eng.*, **3**(2), 195-202. https://doi.org/10.12989/gae.2023.33.2.195.

Liu, P.L. and Der Kiureghian, A. (1986), "Multivariate distribution models with prescribed marginals and covariances", *Probab. Eng. Mech.*, **1**(2), 105-112. https://doi.org/10.1016/0266-8920(86)90033-0.

Low, B.K. (2005), "Reliability-based design applied to retaining walls", *Geotechnique*, **55**(1), 63-75. https://doi.org/10.1680/geot.2005.55.1.63.

Low, B.K. and Tang, W.H. (2007), "Efficient spreadsheet algorithm for first-order reliability method", *J. Eng. Mech.*, **133**(12), 1378-1387. https://doi.org/10.1061/(ASCE)0733-9399(2007)133:12(1378).

Low, B.K. (2020), *Geotechnical Insights from Reliability-Based Design to Improve Partial Factor Design Methods*, 686-695. https://doi.org/10.1061/9780784482797.067.

Lu, Z.H., Cai, C.H. and Zhao, Y.G. (2017), "Structural reliability analysis including correlated random variables based on third-moment transformation", *J. Struct. Eng.*, **143**(8), 04017067. https://doi.org/10.1061/(asce)st.1943-541x.0001801.

Lu, Z.H., Cai, C.H., Zhao, Y.G., Leng, Y. and Dong, Y. (2020), "Normalization of correlated random variables in structural reliability analysis using fourth-moment transformation", *Struct. Saf.*, **82**, 101888. https://doi.org/10.1016/j.strusafe.2019.101888.

Mahmood, Z. (2020), "Reliability-based optimization of geotechnical design using a constrained optimization technique", *SN Appl. Sci.*, **2**(2), 168. https://doi.org/10.1007/s42452-020-1948-4.

Meng, D., Yang, S., He, C., Wang, H., Lv, Z., Guo, Y. and Nie, P. (2022), "Multidisciplinary design optimization of engineering systems under uncertainty: A review", *Int. J. Struct. Integrity*, **13**(4), 565-593. https://doi.org/10.1108/IJSI-05-2022-0076.

Najafizadeh, A. and Zad, A. (2022), "Experimental evaluation of back-to-back anchored walls by double-plates anchors", *Geomech. Eng.*, **31**(6), 599-614. https://doi.org/10.12989/gae.2022.31.6.599.

Negussey, D., Wijewickreme, W.K.D. and Vaid, Y.P. (1988), "Constant-volume friction angle of granular materials", *Can. Geotech. J.*, **25**(1), 50-55. https://doi.org/10.1139/t88-006.

Open TURNS. (2021), *Open Treatment of Uncertainties, Risk's aNd Statistics, an open source source platform*. https://openturns.github.io/www/

Park, K., Kim, D., Park, J. and Na, H. (2021), "The determination of pullout parameters for sand with a geogrid", *Appl. Sci., (Switzerland)*, **11**(1), 1-16. https://doi.org/10.3390/app11010355.

Phoon, K.K. and Ching, J. (2015), *Risk and Reliability in Geotechnical Engineering* (Eds., K.K. Phoon and J. Ching), CRC Press.

Phoon, K.K. and Kulhawy, F.H. (1999), "Characterization of geotechnical variability", *Can. Geotech. J.*, **36**(4), 612-624. https://doi.org/10.1139/t99-038.

Powell, M.J.D. (1994), "A direct search optimization method that models the objective and constraint functions by linear interpolation", (Eds., S. Gomez and J. Pierre Hennart), *Advances in Optimization and Numerical Analysis*, 51-67. Springer, Dordrecht. https://doi.org/10.1007/978-94-015-8330-5_4.

Powell, M.J.D. (1998), "Direct search algorithms for optimization calculations", *Acta Numerica*, **7**, 287-336. https://doi.org/10.1017/S0962492900002841.

Safaee, A.M., Mahboubi, A. and Noorzad, A. (2021), "Experimental investigation on the performance of multi-tiered geogrid mechanically stabilized earth (MSE) walls with wrap-around facing subjected to earthquake loading", *Geotext. Geomembranes*, **49**(1), 130-145. https://doi.org/10.1016/j.geotexmem.2020.08.008.

Schweckendiek, T. (2021), "Model uncertainties in foundation design", *Georisk: Assessment and Management of Risk for Engineered Systems and Geohazards*, **15**(4), 336-336. https://doi.org/10.1080/17499518.2021.1952614.

Tahamtan, J., Gholhaki, M., Najjarbashi, I., Hossaini, A. and Pirmoghan, H. (2024), "Damage rate assessment of cantilever RC walls with backfill soil using coupled Lagrangian-Eulerian simulation", *Geomech. Eng.*, **36**(3), 231-245. https://doi.org/10.12989/gae.2024.36.3.231

Tang, C. and Phoon, K.K. (2018), "Evaluation of model uncertainties in reliability-based design of steel H-piles in axial compression", *Can. Geotech. J.*, **55**(11), 1513-1532. https://doi.org/10.1139/cgj-2017-0170.

Verdugo, R. and Ishihara, K. (1996), "The steady state of sandy soils", *Soils Found.*, **36**(2), 81-91. https://doi.org/10.3208/sandf.36.2_81.

Wang, Q. and Owens, P. (2022), "Reliability-based design optimisation of geotechnical systems using a decoupled approach based on adaptive metamodels", *Georisk*, **16**(3), 470-488. https://doi.org/10.1080/17499518.2021.1884884.

Wolff, T.F. (1994), *Evaluating the reliability of existing levees, Technical report.*

Yalcin, Y., Orhon, M. and Pekcan, O. (2019), "An automated approach for the design of mechanically stabilized earth walls incorporating metaheuristic optimization algorithms", *Appl. Soft Comput. J.*, **74**, 547-566. https://doi.org/10.1016/j.asoc.2018.09.039.

Zhang, H., Wang, H., Wang, Y. and Hong, D. (2019), "Incremental shifting vector and mixed uncertainty analysis method for reliability-based design optimization", *Struct. Multidiscip. O.*, **59**(6), 2093–2109. https://doi.org/10.1007/s00158-018-2178-x.

Zheng, J. and Li, L. (2024), "Experimental and numerical study on the earth pressure coefficient in a vertical backfilled opening", *Geomech. Eng.*, **36**(3), 217-229. https://doi.org/10.12989/gae.2024.36.3.217.

IC